Distribution Agreement

In presenting this thesis as a partial fulfillment of the requirements for a degree from Emory University, I hereby grant to Emory University and its agents the non-exclusive license to archive, make accessible, and display my thesis in whole or in part in all forms of media, now or hereafter now, including display on the World Wide Web. I understand that I may select some access restrictions as part of the online submission of this thesis. I retain all ownership rights to the copyright of the thesis. I also retain the right to use in future works (such as articles or books) all or part of this thesis.

Yeer Jin March 27, 2023

Determining the impact of the RGS14-Gαi1-GDP complex on NHERF1 binding

by

Yeer Jin

Dr. John R. Hepler

Adviser

Neuroscience and Behavioral Biology

Dr. John R. Hepler

Adviser

Dr. Leah Roesch

Committee Member

Dr. Randy Hall

Committee Member

Dr. Joseph Manns

Committee Member

2023

Determining the impact of the RGS14-Gαi1-GDP complex on NHERF1 binding

By

Yeer Jin

Dr. John R. Hepler

Adviser

An abstract of

a thesis submitted to the Faculty of Emory College of Arts and Sciences of Emory University in partial fulfillment

of the requirements of the degree of

Bachelor of Science with Honors

Neuroscience and Behavioral Biology

2023

Abstract

Determining the impact of the RGS14-Gαi1-GDP complex on NHERF1 binding
By Yeer Jin

Regulator of G Protein Signaling 14 (RGS14) is a multifunctional signaling protein that integrates G protein, mitogen-activated kinase/extracellular regulated kinase (MAPK/ERK), and Ca^{++}/CaM signaling pathways. Expressed in human hippocampal CA2 pyramidal cells, RGS14 plays a vital role in suppressing synaptic plasticity and long-term potentiation in the context of hippocampal-related memory. Human RGS14 contains an RGS domain that binds to Gαi/o-GTP, a tandem Ras/Rap binding domain (RBD) that binds active H-Ras/Rap2-GTP, a GRP motif that binds to Gαi1/3-GDP, and a poorly characterized PDZ-binding motif. While much is known about the RGS domain, RBD, and GPR motif using rodent models, little is known about the PDZ-binding motif due to its absence in rodent RGS14.

Recent findings show that human RGS14 binds to NHERF1, a PDZ domain containing scaffolding protein located in postsynaptic spines, where it regulates GPCR-G signaling. RGS14 is well positioned to regulate both NHERF1 and Gαi1signaling at the plasma membrane. However, NHERF1 via its PDZ2 domain and Gαi1-GDP each bind RGS14 in very close proximity. How the binding of one protein impacts the binding of the other is unknown. In order to understand the interaction between the three proteins, we examined their direct binding as purified proteins. Using co-immunoprecipitation of human RGS14 with Gαi1-GDP, NHERF1, and the isolated PDZ2 domain of NHERF1, we tested the relative ratio and competition for successful binding between human RGS14, Gαi1-GDP, and the PDZ2 domain. The results suggested the importance of the order of protein binding for complex formation, as the binding of Gαi1-GDP first to human RGS14 reduces the apparent affinity of the PDZ2 domain towards the dimer. These findings imply a Gi-mediated mechanism for the regulation of the subcellular localization of RGS14 and NHERF1 and complex formation. Overall, our findings implicate RGS14 as an intermediate regulator of both NHERF1 and Gαi1 signaling in brain, providing more insights into its coupling mechanisms. Future studies will explore the impact of NHERF1 binding on RGS14-Gαi1-GDP complex formation (and vice versa) as purified proteins using size-exclusion chromatography and in live cells using BRET analysis.

Determining the impact of the RGS14-Gαi1-GDP complex on NHERF1 binding

By

Yeer Jin

Dr. John R. Hepler

Adviser

A thesis submitted to the Faculty of Emory College of Arts and Sciences

Of Emory University in partial fulfillment

of the requirements of the degree of

Bachelor of Science with Honors

Neuroscience and Behavioral Biology

2023

Acknowledgments

I would like to thank all members of the Hepler Lab for their support. I would like to particularly thank Suneela Ramineni for training me when I joined the lab and teaching me protein purification, size-exclusion column, SDS-PAGE gels, co-IP, and Western blotting. Suneela Ramineni also helped me with the experiment design and troubleshooting. I am very thankful for the opportunity to participate in the Hepler Lab, where I learned and practiced research in a challenging yet educational setting.

I would like to thank my committee members, Drs. Leah Roesch, Randy Hall, and Joseph Manns, for their support and valuable input during my honors thesis. My undergraduate journey in neuroscience had been incredible, with a solid foundation and extended learning thanks to these inspiring figures.

I would like to thank my family members, including my parents Fang Ye and Zhibin Jin, my cousin Feier Mo, my grandmother Jieru Wei, and my great-grandmother Huihui Zhang, for their constant emotional support and love in Los Angeles and Shaoxing, China.

I would like to thank my lovely furry family members, Boba and Kaia the twin cats (my favorites), Sunshine the Golden Doodle, Latiao the Jack Russell Terrier, and Nuomi the white cat. Without their constant influx of photos and videos, I would be miserable and have no pictures for my phone and laptop wallpapers.

I would also like to thank my friends Celine Lyu, Celina Gao, Joyce Wang, Ashley Lou, and Jing Li for their emotional support and role as meal or FaceTime buddies. Their remembrance of me in daily life kept me sane and motivated.

Finally, I would like to give my deepest gratitude to my advisor, Dr. John Hepler, for his patient guidance, enthusiastic encouragement, and helpful feedback on this research work. This project would not have been possible without his trust and guidance, even when I didn’t believe in myself.

This project was funded by1 R01 GM140632-01.

Table of Contents

Illustrations

INTRODUCTION

G protein coupled receptors (GPCR) are the most prominent family of cell surface receptors, which play an essential role in central nervous system neurotransmission through their expression in presynaptic and postsynaptic terminals (Betke et al., 2012). GPCRs are seven membrane-spanning α-helical proteins that bind to specific extracellular ligands such as single photons, hormones, neurotransmitters, and proteolytic enzymes (Millar and Newton, 2010; Betke et al., 2012). Following the conformational change of GPCR caused by ligand binding, the exchange of GDP to GTP occurs, and the Gα subunit of GPCR dissociates from the Gβγ complex (Brown et al., 2015a). The subunits then separately lead to the downstream signaling cascades that influence a wide range of components within the neurotransmission pathway (Betke et al., 2012). Ultimately, when GTPase promotes GTP hydrolysis through binding with the Gα subunit, the downstream signaling will be turned off, and GPCRs' influence will be terminated (Betke et al., 2012; Harbin et al., 2021).

The regulators of the G-Protein signaling (RGS) family of proteins play a role in this control of GPCRs neurotransmission by modulating the lifetime of bound GTP on the Gα subunit, therefore accelerating the turn-off of the downstream signaling eventually (Hollinger and Hepler, 2002; Gerber et al., 2016; Harbin et al., 2021). This is done by the presence of an RGS domain, which binds to the G protein and functions as a GTPase-activating protein (GAP) that accelerates the GTP hydrolysis during the termination process (Zheng et al., 1999; Brown et al., 2015a). The capacity of RGS proteins to accelerate the turn-off of downstream signaling events inside the cell is crucial in synaptic plasticity (Chen and Lambert, 2000; Goldenstein et al., 2009; Talbot et al., 2010).

RGS14 and its binding partners in the brain

RGS14 is a multifunctional RGS protein belonging to the R12 family (Harbin et al., 2021; Gerber et al., 2016). With studies of RGS14 primarily focusing on the rodent model, it is now known that RGS14 is highly expressed in discrete regions of the rodent brain such as the hippocampal CA2 area, basal ganglia, and nucleus accumbens, implying its more targeted function (Evans et al., 2014; Harbin et al., 2021; Squires et al., 2018; Montanez, Bramlett, 2023). RGS14 is specifically present in the hippocampal CA2 pyramidal cell bodies, axons, and dendrites and scarcely in the CA1 region, and CA2 pyramidal cells inhibit long-term potentiation (LTP), aid the formation of social memory, and play an essential role in the epileptic network (Lee et al., 2010; Caruana et al., 2012; Evans et al., 2015; Chevaleyre and Piskorowski, 2016; Häussler et al., 2016; Tzakis and Holahan, 2019). Studies have shown the presence of RGS14 participating in these functions, where it regulates the suppression of LTP in the mechanism of learning and memory consolidation and also serves a neuroprotective role against CA2 cell death after epilepsy (Lee et al., 2010).

RGS14 mediates post-synaptic signaling and neuronal plasticity by interacting with G protein, mitogen-activated kinase/extracellular regulated kinase (MAPK/ERK), and calcium signaling pathways (**Fig. 1**) (Harbin et al., 2021). The RGS domain of RGS14 binds to the Gα-GTP subunit and accelerates the GTP hydrolysis , thus decreasing the downstream signaling pathway (Harbin et al., 2021). RGS14 also has a tandem Ras/Rap binding domain that regulates MAP kinase signaling (Shu et al., 2010). There are also two tandem Ras binding domains called the R1 and R2 domains, which interact with H-Ras-GTP and Rap2-GTP proteins to hydrolyze GTP (Traver et al., 2000; Vellano et al., 2013). The R1/R2 domain also interacts with calcium/calmodulin (Ca^{2+}/CaM) and Ca^{2+}/CaM kinase II (CaMKII) at unknown sites (Evans et

al., 2018). The G-protein Regulatory motif (GPR) binds to inactive Gαi1/3-GDP protein, inhibiting the dissociation of GDP and the exchange of GTP for activation and promoting the stable blinding of RGS14 to the plasma membranes (Brown et al., 2015). In the linker region between the RGS and R2 domains, there is a nuclear localization sequence (NLS) and a nuclear export sequence (NES) in the GPR domain that regulate RGS14 nucleo-cytoplasmic shuttling for unknown functions (Harbin et al., 2021).

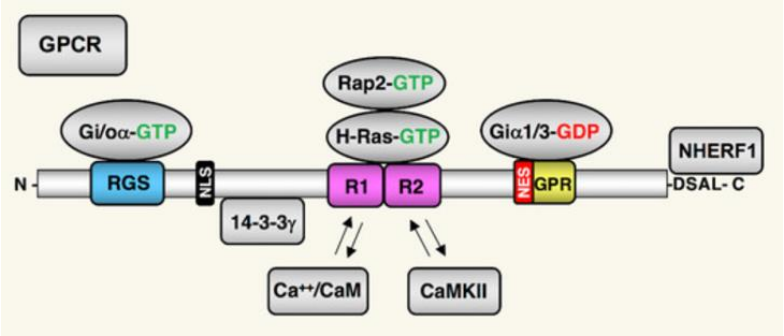

Figure 1. Human RGS14 structural model and its various binding partners. (See text)

Human RGS14 binds NHERF1

While rodent RGS14 has been studied extensively, RGS14 expression in primate brains had not been explored to a similar degree. Recent studies in rhesus macaques and humans indicate that human RGS14 differs from rodent protein in its protein expression pattern and specific biochemical properties (Squires et al., 2018; Friedman et al., 2019). Through studies in rhesus macaques, the expression of RGS14 in the hippocampal regions is similar to the rodent models, but its expression is strong in both CA2 pyramidal cells and CA1 region's pre- and post-synaptic regions in the neuropil, pyramidal cell bodies, and proximal dendritic profile (Squires et al., 2018; Harbin et al., 2021; Montanez-Miranda et al., 2023). This expression indicates RGS14's role in hippocampal-based learning and memory, similar to past studies with rodent models (Harbin et al., 2021). However, its expression is also highly significant in

immunoreactivity at other regions, such as the caudate nucleus, putamen, substantia nigra pars reticulata, Globus pallidus, and it's also expressed moderately in the amygdala and nucleus accumbens (Squires et al., 2018; Montanez-Miranda et al., 2023). Aside from the brain, RGS14 is expressed in the human heart, kidney, immune system (macrophages), and adipose tissue (Beadling et al., 1999; Mittmann et al., 2002; Vatner et al., 2018; Harbin et al., 2021; Friedman et al., 2022a). Unlike rodent RGS14, human RGS14 contains an additional 22 amino acids at its C-terminus, which includes a PDZ binding motif (-DSAL). (Friedman et al., 2019; Harbin et al., 2021). This PDZ binding motif has been shown to interact with the PDZ scaffold protein sodium hydrogen exchanger regulatory factor-1 (NHERF1) protein on its PDZ2 domain in the human kidney, regulating NPT2A/NHERF1 complex and phosphate homeostasis in the proximal kidney tubule (Friedman et al., 2019, 2022a).

NHERF1 regulates mGluR2/3 signaling in brain

NHERF1 is a scaffolding protein that contains two tandem PDZ domains and an ezrin-radixin-moesin (ERM)-binding domain in the C terminus, and its role in regulating GPCR-G protein signaling has been widely studied (Brône and Eggermont, 2005; Ardura and Friedman, 2011). In the rat and human brain, NHERF1 is expressed throughout the hippocampal regions, with its expression highly significant in the human hippocampus from the other brain region (**Fig. 2**). However, it is expressed the most significant in the dentate gyrus and also in the CA1 and CA2 areas, where RGS14 is present in human brain (Allen Institute for Brain Science). NHERF1 is known to interact with mGluR2/3's PDZ-binding motif at the C terminus in the CA2 pyramidal cells to regulate their functions (Ritter-Makinson et al., 2017; Harbin et al., 2021).

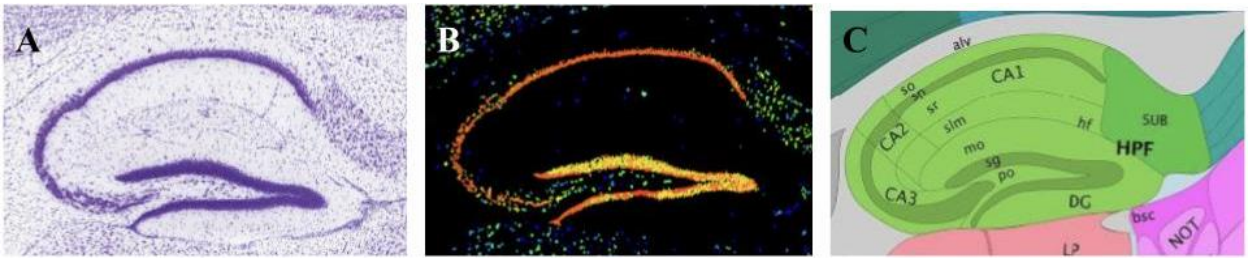

Figure 2. NHERF1 expression patterns and projection of NHERF1-expressing neurons in the hippocampal region. A: Nissl annotation of NHERF1-expression neurons from Allen Mouse Brain Atlas. Allen Mouse Brain Atlas, mouse.brain-map.org/gene/show/26686. B. Expression annotation of NHERF1 from Allen Mouse Brain. Allen Mouse Brain Atlas, mouse.brain-map.org/gene/show/26686. C. Anatomical annotation from the Allen Reference Atlas - Mouse Brain at the same slice position as A and B. Allen Mouse Brain Atlas and atlas.brain-map.org.

mGluR2/3 are group II metabotropic glutamate receptors with seven transmembrane domains that regulate neurotransmitter release and excitatory synaptic potentials and activity-dependent modification of synaptic plasticity (Blümcke et al., 1996; Ferraguti and Shigemoto, 2006; D'Antoni et al., 2008). These receptors are expressed in rat brain regions that include the cerebellum, dentate gyrus granule cells, the olfactory bulb, the thalamus, the cortex, and the hippocampus (Bodzęta et al., 2021). mGluR2/3 each couple to Gi/o to negatively regulate adenylate cyclase and cAMP signaling (Pin and Duvoisin, 1995; D'Antoni et al., 2008; Ritter and Hall, 2009). mGluR2/3 have been extensively studied as potential targets for the treatment of various neurodegenerative and neuropsychiatric disorders, such as schizophrenia, depression, Parkinson's disease, Alzheimer's disease, and drug addiction (Vinson and Conn, 2012; Nicoletti et al., 2015; Abd-Elrahman et al., 2023). In the brain, they are highly expressed in human hippocampal astrocytes and present in the human CA2 pyramidal cells (Blümcke et al., 1996; D'Antoni et al., 2008). mGluR2/3 were thought to play a role in regulating long-term potentiation in the Schaffer collateral-CA1 pyramidal cell synapses by priming NMDA receptors in the brain, which implies their potential importance in learning and memory (Pin and Duvoisin,

1995; Rosenberg et al., 2016). They also have a neuroprotective role against glutamate-induced excitotoxicity that causes neuronal and glial cell death (Pin and Duvoisin, 1995).

When coupling with NHERF1, mGluR2 binds to both PDZ1 and PDZ2 domains in NHERF1, and mGluR3 specifically binds to the PDZ1 domain in NHERF1 and only weakly to the PDZ2 domain (Ritter-Makinson et al., 2017). The binding of mGluR2/3 and NHERF1 led to cellular localization and expression in the perisynaptic astrocyte process (PAP) (Ritter-Makinson et al., 2017). Studies have shown that the binding of NHERF1 to the C-tail of mGluR2 and mGluR3 regulates the distribution of mGluR2/3 receptors in the axons of the prefrontal cortex (Ritter-Makinson et al., 2017). At the same time, mGluR2/3 proteins are known to bind with both Gαi1/3 and NEHRF1, which also interact with RGS14 at its GPR motif and PDZ motif, respectively (Harbin et al., 2021; Lin et al., 2021; Seven et al., 2021).

Working hypothesis and goals for these studies

RGS14 binds Gαi1-GDP at the GPR motif near its C-terminus to inhibit the dissociation of GDP and the exchange of GTP for activation (Hollinger et al., 2001; Shu et al., 2010). At the same time, RGS14 also binds to NHERF1 at the C-terminal PDZ binding motif, only 18 amino acids away (**Fig. 3**) (Harbin et al., 2021; Friedman et al., 2022a). Since RGS14 binds both Gαi1-GDP and NHERF1, which are all present in the CA2 pyramidal cells, the central question of this study is to determine if RGS14 binding to either Gαi1-GDP or NHERF1 impacts the binding of other protein (**Fig. 2**) (Blümcke et al., 1996; Harbin et al., 2021). That is, can RGS14 bind both Gαi1-GDP and NEHRF1 simultaneously, or does the binding exclude binding of the other due to potential steric hindrance caused by the proximity between the GPR motif and the PDZ-binding motif? Since RGS14 utilizes the binding of Gαi1-GDP as a mechanism for plasma membrane

localization (Brown et al., 2015a), these studies will determine how the RGS14-Gαi1-GDP complex impacts NHERF1 binding and membrane localization to modulate its functions.

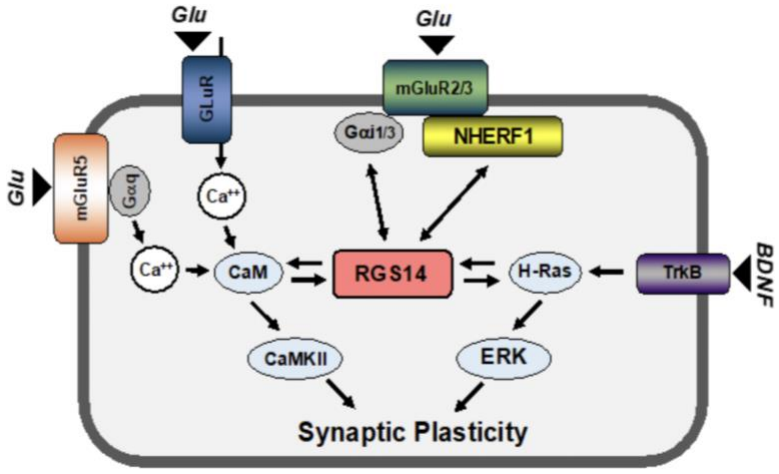

Figure 3. Working model of human RGS14 regulation of mGluR2/3-Gi-NHERF1 signaling in hippocampal CA1/CA2 neurons. (see text above and in discussion)

METHODS

Protein Transformation

Competent cells Bl21(DE3) were used for protein expression. 200ng of DNA (1uL) for expressing the protein of interest was added to a 15 mL culture tube, and 50 uL of competent cells were added into the tube and mixed well by swirling and tapping on the tube. The solution was incubated on ice for 30 minutes. After 30 minutes, the solution was heat shocked at 42℃ for 40 seconds, and it was then incubated on ice for another 2 minutes. Ensuring all surfaces were cleaned with 70% ethanol, 200uL of NZYT+ was added into the tube. The tube was then incubated in the shaker incubator for 60 minutes at 37℃. Meanwhile, an agar plate with Carbenicillin was prepared by drying it in the incubator at 37℃. After amplification, 50 uL of the culture was added and spread onto the plate, which was then incubated overnight at 37℃ in

the incubator. A colony was then picked to be expressed in LB + Carbenicillin, and the cells were stored as a glycerol stock for future protein expression.

His6-Gai Protein Expression and Purification

H6-Gαi were expressed in Bl21(DE3) competent cells in LB + Carbenicillin, and the protein expression was induced by IPTG at 20 degrees overnight. The pellet was resuspended in 50mM HEPES, 200mM NaCl, 20mM Imidazole, 10% Glycerol, 2mM BME, 1% Triton X and some protease inhibitors. Lysosome and DNase were added to the pellet, and the mixture was sonicated. The cell lysate was resuspended in 50mM HEPES, 200mM NaCl, 20mM Imidazole, 10% Glycerol, 2mM BME, 1% Triton X and some protease inhibitors. After removing debris and DNA by the Ti45 rotor, the protein was purified by Ni-NTA columns and washed with buffer after repeating the columns. The protein was eluted from the resin by 50mM HEPES, 200mM NaCl, 200mM Imidazole, 1x PMSF, and 2mM BME. The eluates with a concentration higher than 0.1 mg/mL were mixed and dialyzed in a solution containing 50mM HEPES, 100mM NaCl, 0.5mM (1M) DTT, 1mM (.5M) EDTA, 1uM (130 mM) GDP overnight. The load, flowthrough, wash, elute, predialyzed elute mixture, and the dialyzed eluted protein was run on SDS-PAGE Gel.

His6-NHERF1 Protein Expression and Purification

H6-NHERF1 were expressed in Bl21(DE3) competent cells in LB +Carbenicillin, and the protein expression was induced by IPTG at 20 degrees overnight. The pellet was resuspended in 50mM HEPES, 200mM NaCl, 20mM Imidazole, 10% Glycerol, 2mM BME, 1xPMSF, and some protease inhibitors. Lysosome was added to the pellet, and the mixture was French pressed for 2-

3 times. The cell lysate was then resuspended in 50mM HEPES, 200mM NaCl, 20mM Imidazole, 10% Glycerol, 2mM BME, 1xPMSF, and some protease inhibitors. After the removal of debris and DNA by the Ti45 rotor, the protein was purified by Ni-NTA columns and washed with buffer after repeating the columns. The protein was eluted from the resin by 50mM HEPES, 200mM NaCl, 200mM Imidazole, 1x PMSF, and 2mM BME. The load, the flowthrough, the wash, and the eluted protein was run on SDS-PAGE Gel.

His6-MBP-TEV-human RGS14 Protein Expression and Purification

MBP-TEV-RGS14 were expressed in Bl21(DE3) competent cells in LB +Carbenicillin, and the protein expression was induced by IPTG at 20 degrees overnight. The pellet was resuspended in 50mM HEPES, 200mM NaCl, 20mM Imidazole, 10% Glycerol, 2mM BME, 1xPMSF, and some protease inhibitors. Lysosome was added to the pellet, and the mixture was French pressed 2-3 times. The cell lysate was resuspended in 50mM HEPES, 200mM NaCl, 20mM Imidazole, 10% Glycerol, 2mM BME, 1xPMSF, and some protease inhibitors. After removing debris and DNA by the Ti45 rotor, the protein was purified by Ni-NTA columns and washed with buffer after repeating the columns. The protein (Hu-RGS14) was eluted from the resin by 50mM HEPES, 200mM NaCl, 200mM Imidazole, 1x PMSF, and 2mM BME. The load, the flowthrough, the wash, and the eluted protein was run on SDS-PAGE Gel.

The purified protein was concentrated in 2 mL for purification through size exclusion chromatography. By using FPLC with a S75 and S200 columns back-to-back, the protein was run in a buffer of 50mM HEPES, 150mM NaCl, and 2mM DTT. After eluting the proteins in fractions of 500uL, 20uL of proteins was mixed with 40uL of 2x sample buffer. The samples were then heated for 5 minutes and ran through an SDS-PAGE gel with load and ladder.

Co-Immunoprecipitation of Hu-RGS14 and its binding partners

Hu-RGS14, the proteins of interest were added together with assay buffer (1xPBS with 2mM MgCl2 and 50uM of GDP), forming a 448 uL solution. The solution was incubated for 60 minutes on rotation at 4℃. During the incubation, 100uL of agarose beads were washed twice with 1mL of 1xTBS at low speed. 3% BSA in 1x PBS solution was added to block the beads, which were incubated at 4℃ by rotating for 3 hours. After 1 hour of protein incubation, 2uL of RGS14 polyclonal antibody was added to the solution, and the tubes were incubated overnight. After 3 hours of blocking, the beads were washed once with 1mL of assay buffer and stored at 4℃.

After the solutions were incubated overnight, it was added into their individual tubes of pre-blocked agarose beads, where the tubes were incubated by rotating for 2 hours at 4℃. After incubation, the beads were washed three times with 500uL of wash buffer, containing 1x TBS with 0.01% Triton X. 100uL of 2x DTT sample buffer was added to each sample, and they were boiled for 5 minutes, where SDS-PAGE gels were run accordingly at 160mV for 1 hour and 40 minutes.

Immunoblotting

The protein bands from previously run SDS-PAGE gels were transferred to a nitrocellulose membrane at 300mA for 2 hours. Membranes were stained with 1:100 ponceau stain stock-to-water dilution to ensure the successful transfer of bands. Ponceau red stain containing 20 mg/mL Ponceau S in water. The membranes were blocked in blocking buffer containing 5% nonfat milk (w/v), 0.1% Tween 20, and 0.02% sodium azide in 20 mm TBS overnight at 4℃, and they were then incubated with primary antibodies in the same buffer for 3

hours at room temperature. Membranes were washed three times for 10, 5, and 5 minutes with TBS containing 0.1% Tween 20 (TBST) before being incubated with anti-mouse HRP-conjugated secondary antibody diluted in TBST with 1:5,000 ratio for 1 hour at room temperate. After the incubation, membranes were washed three times for 10, 5, and 5 minutes in TBST before visualizing protein bands using enhanced chemiluminescence and exposing membranes to X-ray films.

RESULTS

Protein Purification

His6-Gαi-GDP and His6-NHERF1 were purified using Ni-NTA affinity columns. By purifying each protein in two parallel Ni-columns, His6-NHERF1 eluates were collected for future complex studies, and His6-Gαi-GDP eluates with a concentration higher than 0.1 mg/mL were collected and dialyzed with GDP to ensure its stability in the deactivated form. SDS-PAGE gels were run for each protein with its load, flow through, and resulting batches, and the gels were stained using Coomassie stains visualization (**Fig. 4**). The eluate batches were highly concentrated with the correct kDa size of 50 for His6-NHERF1 and 41 for His6-Gαi-GDP.

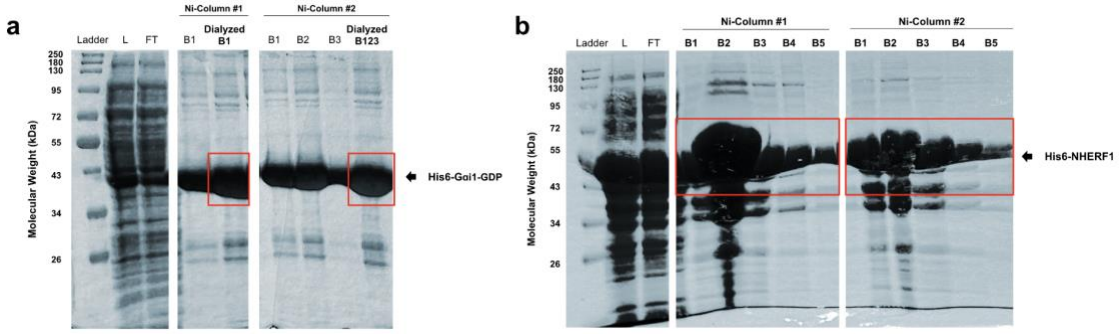

Figure 4. SDS-PAGE of His6-Gαi1-GDP and His-NHERF1 purifications. (a) Purified H6Gαi1-GDP was collected from the NI-NTA column, dialyzed with GDP, and SDS-PAGE of load, pre-dialyzed eluates, and dialyzed eluates were stained with Coomassie blue. (b) Purified H6NHERF1 was collected from the NI-NTA column, and SDS-PAGE of loads and eluates were stained with Coomassie blue. The red boxes indicate all purified proteins.

Human RGS14 (His6-MBP-TEV-RGS14) was purified using similar methods twice, in addition to dialysis with TEV proteas for cleavage of His6-MBP-TEV from the purified Hu-RGS14. After collecting the dialyzed Hu-RGS14, a Ni-NTA column was used to filter out the cleavedHis6-MBP-TEV, and a size exclusion chromatography with S75 and S200 was used to purify the Hu-RGS proteins from TEV protease and leftover His6-MBP-TEV further (**Fig. 5**). The batches containing hu-RGS at approximately 63 kDa were collected for future complex analysis.

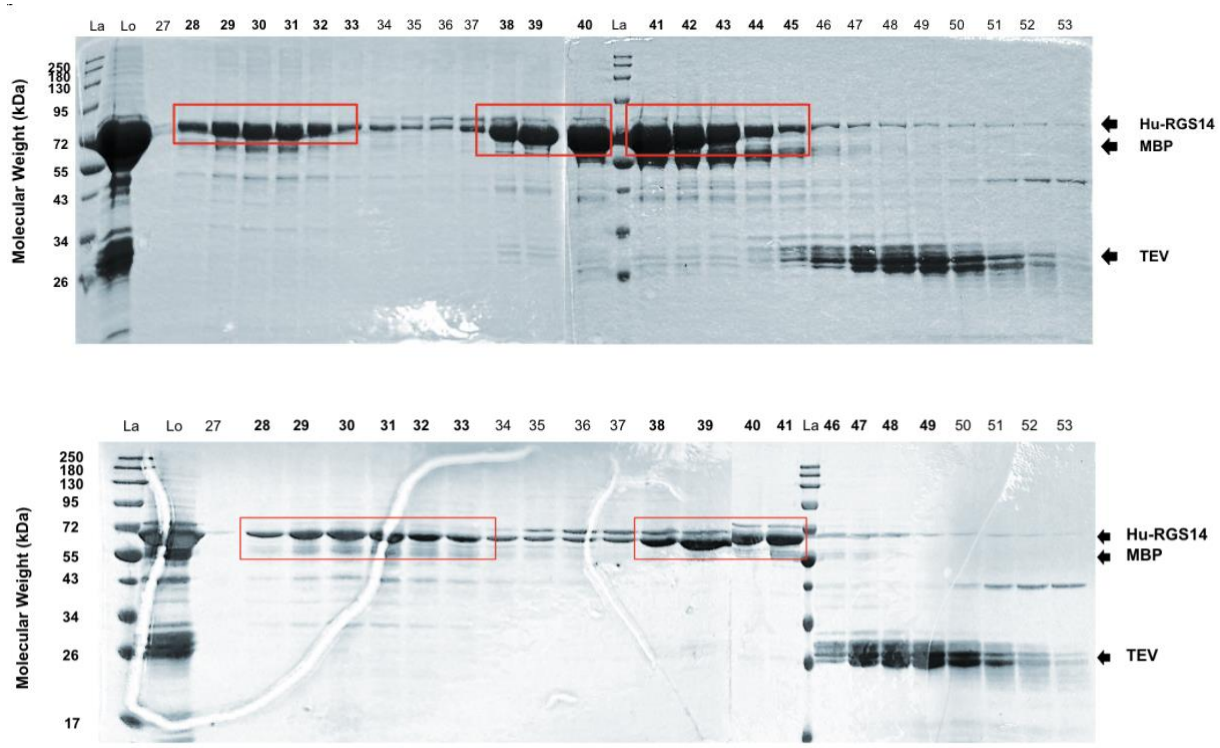

Figure 5. SDS-PAGE of Hu-RGS14 purification. Purified Hu-RGS14 collected from the NI-NTA column was dialyzed with TEV protease and purified again in the NI-NTA column and FPLC. SDS-PAGE of load and specific eluates were stained with Coomassie blue. The red boxes indicate the purified proteins.

Complex Binding

With the purification of proteins of interest, Ni-pulldown was first employed to assess the binding between Hu-RGS14 separately with His6-NHERF1 and His6-Gαi1-GDP. However, the

negative control of Hu-RGS14 alone with beads showing presence in the SDS-PAGE gel results after 3 runs, which was unexpected due to its removed His tag during purification (**Fig. 6**).

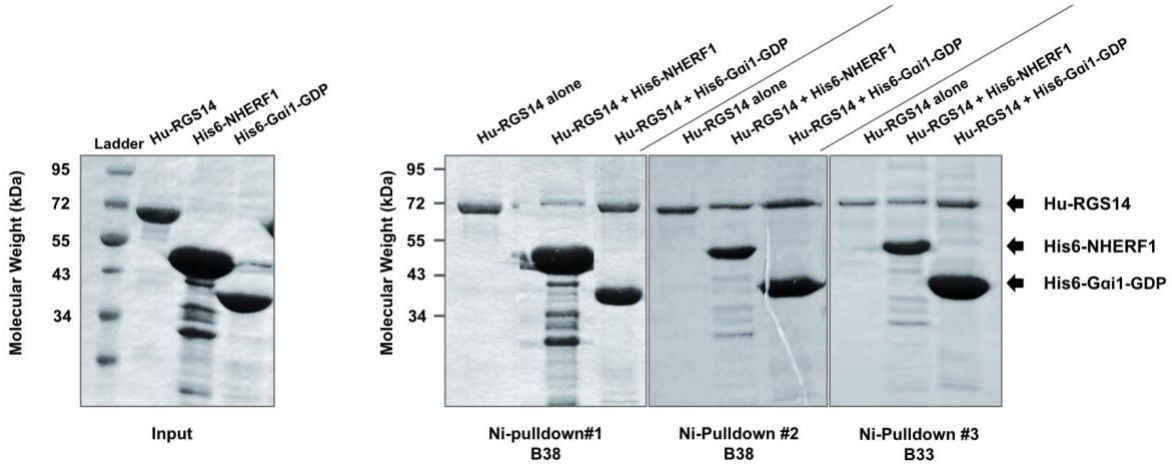

Figure 6. SDS-PAGE of Hu-RGS14 + His6-NHERF1 and Hu-RGS14 + His6-Gαi1-GDP complexes with negative controls of Hu-RGS14 alone in Ni-NTA pulldowns. Hu-RGS14 were separately coupled with His6-NHERF1 and His6-Gαi1-GDP, and coomassie staining was done. With Hu-RGS14 lacking the His-tag, there is still binding with Ni-NTA beads, suggesting potential nonspecific binding between the protein and the beads.

Immunoprecipitation (IP) was then used for more specific results between the interaction. By incubating Hu-RGS14 with either His6-NHERF1 or His6-Gαi1-GDP in a 1:3 ratio, the proteins were precipitated by the RGS14 antibody. Comparing the binding results with negative controls of His6-NHERF1 and His6-Gαi1-GDP alone indicated significant dimerization of Hu-RGS14 with His6-NHERF1 and His6-Gαi1-GDP (**Fig. 7**). The IP result showed a stronger band expression of His6-Gαi1-GDP when coupled Hu-RGS14 than His6-NHERF1 with Hu-RGS14 (**Fig. 7**).

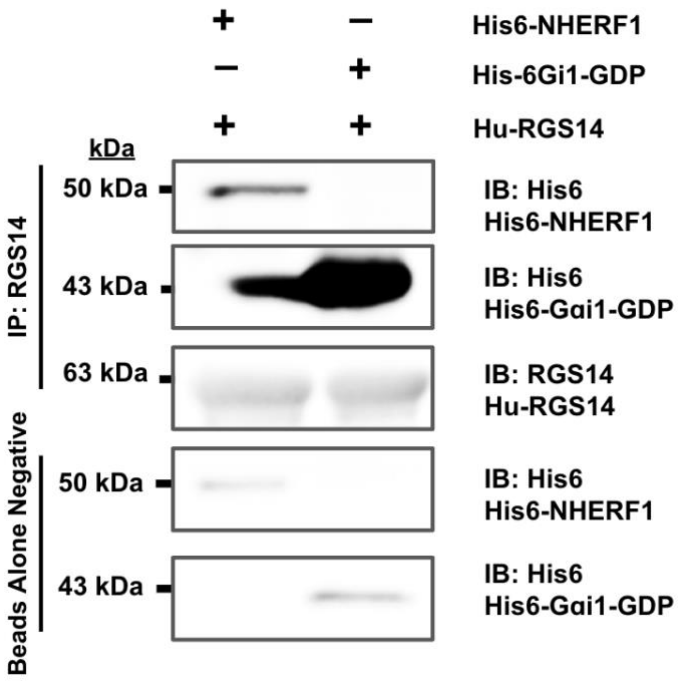

Figure 7. Co-Immunoprecipitation of Hu-RGS14 + His6-NHERF1 and Hu-RGS14 + His6-Gαi1-GDP complexes with negative controls of His6-NHERF1 alone and His6-Gαi1-GDP alone. Hu-RGS14 was separately coupled with His6-NHERF1 and His6-Gαi1-GDP with the addition of the RGS14 antibody. Immunoblot analysis was done with RGS14 antibody to Hu-RGS14 and His6 antibody to His6-NHERF1 and His6-Gαi1-GDP.

To further study the degree of interactions between Hu-RGS14 and NHERF1, 1x of Hu-RGS14 was separately incubated with 3x, 5x, and 10x of His6-NHERF11 and His6-NHERF1 and His6-PDZ2. However, the negative control for 10x His6-NHERF1 alone showed non-specific binding with the RGS14 antibody, as multiple runs with different washing conditions could not achieve a significant reduction in the expression of His6-NHERF1 (**Fig. 8&9**). On the other hand, binding between Hu-RGS14 and 10x His6-PDZ2 indicated a strong binding with Hu-RGS14 despite some technical issues during the procedural process, and its comparison with the negative control of 10x His6-PDZ2 ensured its significance (**Fig. 8**).

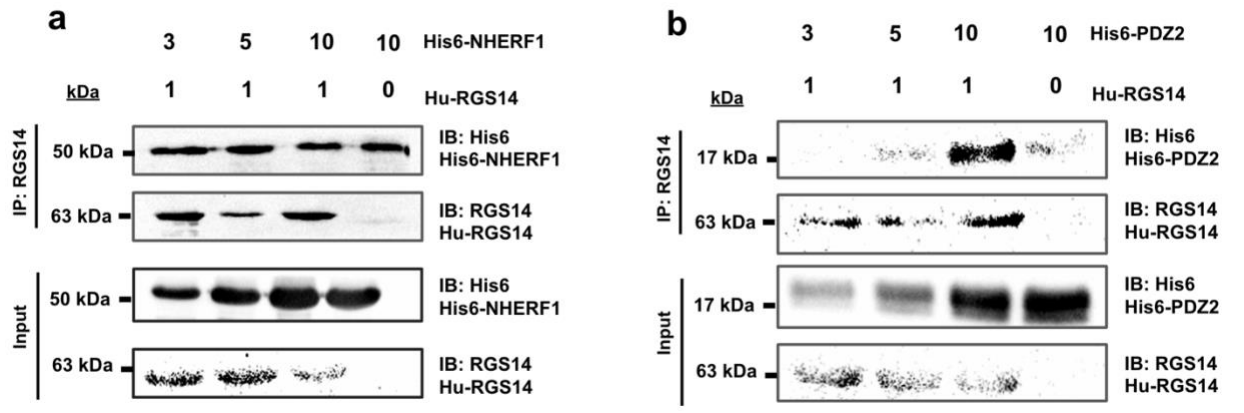

Figure 8. Co-Immunoprecipitation of Hu-RGS14 + His6-NHERF1 and Hu-RGS14 + His6-PDZ2 complexes with negative controls of his6-NHERF1 alone and His6-PDZ2 alone. Hu-RGS14 was separately coupled with (a) His6-NHERF1 and (b) His6-PDZ2 with the addition of the RGS14 antibody. Immunoblot analysis was done with RGS14 antibody to Hu-RGS14 and His6 antibody to His6-NHERF1 and His6-PDZ2. (a) Consistent binding between the RGS14 antibody and NHERF1 was seen with its negative control. (b) Specific binding between Hu-RGS14 and His6-PDZ2 in a ratio of 1:10 was indicated with the reassurance of its negative binding result.

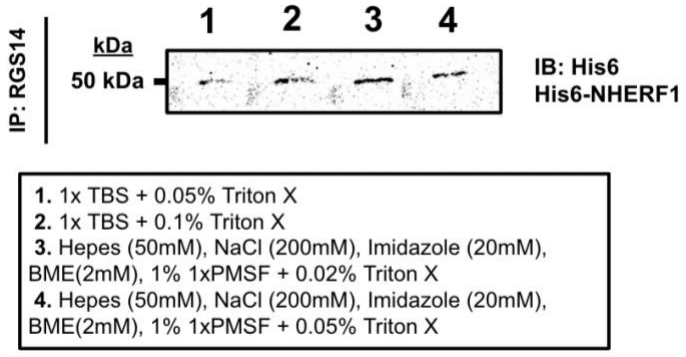

Figure 9. Immunoprecipitation of His6-NHERF1 alone with RGS14 antibody under 4 washing conditions. With different washing conditions, His6-NHERF1 were all present in similar band signals, indicating a specific binding between NHERF1 and RGS14 antibody.

With the difficulties of separating the nonspecific binding of 10x His6-NHERF1 with RGS14 antibody, the intended Co-IP studying the complex formation of Hu-RGS14 + His6-NHERF1 + His6-Gαi1-GDP was therefore modified into Hu-RGS14 + His6-PDZ2 + His6-Gαi1-GDP due to promising data showing the consistent binding between PDZ2 and Hu-RGS14. To further study the level of interaction with the potential hindrance in simultaneous binding, 1x

Hu-RGS14 was coupled with 10x His6-PDZ2 and 3x His6-Gαi1-GDP in a different order, with each new addition of His6-PDZ2 or His6-Gαi1-GDP taking 1 hour of incubation. Initially, His6-PDZ2 was diluted with assay buffer in a 1:2 ratio into 5 µL, which failed to take present in the complex coupling despite clear interaction between Hu-RGS14 and His6-Gαi1-GDP (**Fig. 10**). After using the same 5 µL of non-diluted His6-PDZ2, there was a significant complex formed between the three proteins as compared to their individual negative controls (**Fig. 11**).

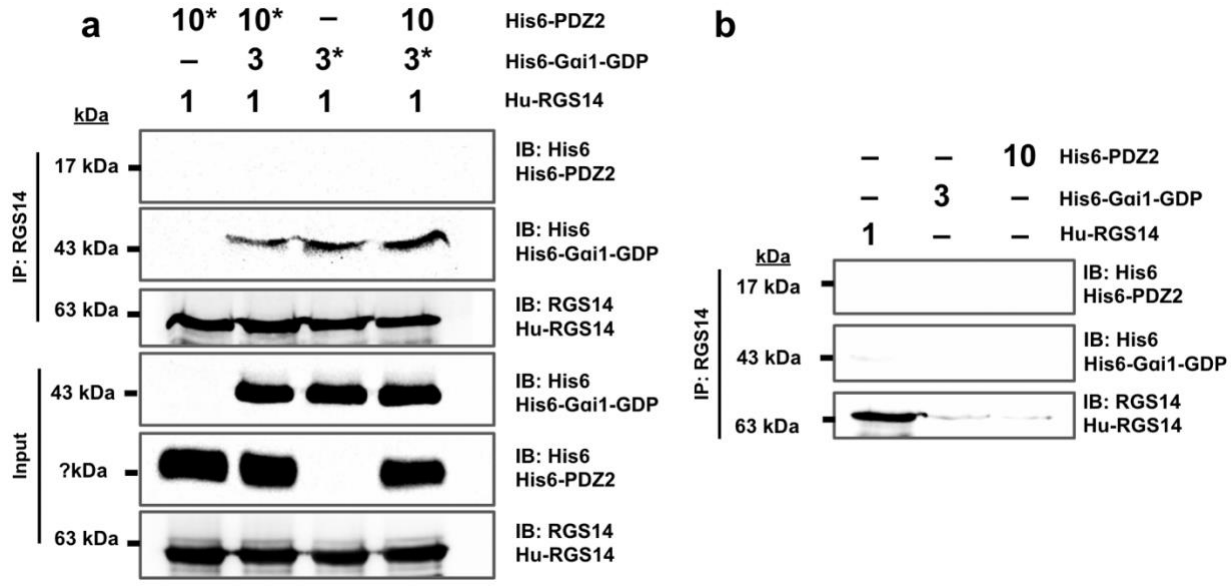

Figure 10. Co-Immunoprecipitation of Hu-RGS14 + His6-His6-PDZ + His6-Gαi1-GDP with different incubation order of His6-NHERF1 and His6-Gαi1-GDP. Hu-RGS14 was coupled with His6-PDZ2 and His6-Gαi1-GDP in a ratio of 1:10:3 and different incubation order with the addition of the RGS14 antibody. Immunoblot analysis was done with RGS14 antibody to Hu-RGS14 and His6 antibody to His6-PDZ2 and His6-Gαi1-GDP. (a) While His6-Gαi1-GDP remains consistent binding regardless of its incubation order, there is no His6-PDZ binding with Hu-RGS14 in all conditions. The asterisk* indicates the first protein being incubated with Hu-RGS14.

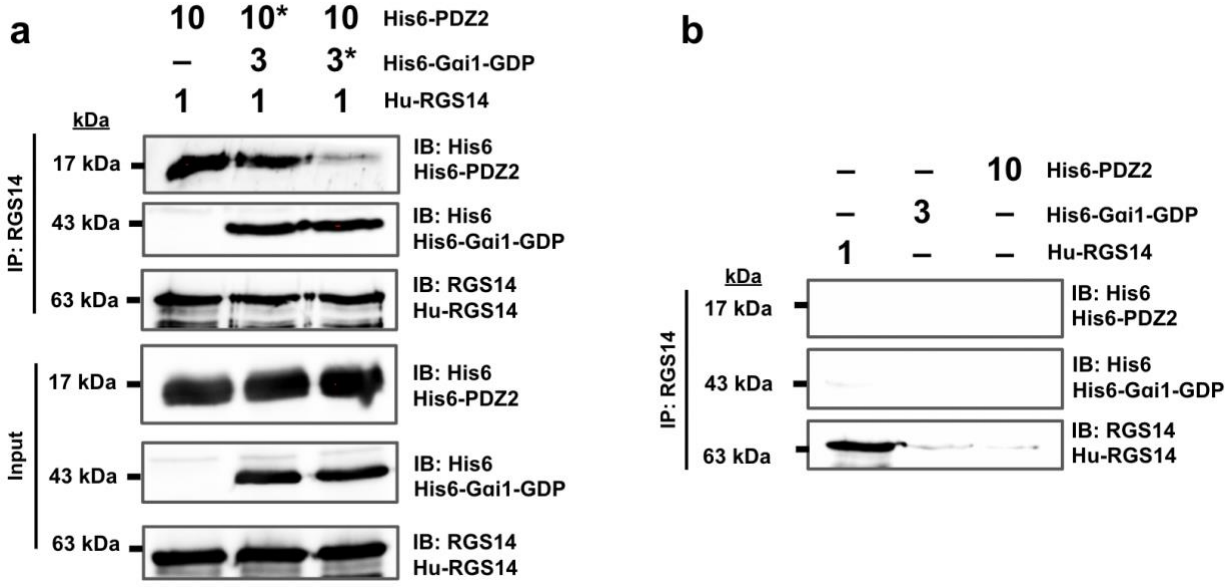

Figure 11. Co-Immunoprecipitation of Hu-RGS14 + His6-His6-PDZ (non-diluted) + His6-Gαi1-GDP with different incubation order of His6-NHERF1 and His6-Gαi1-GDP. Hu-RGS14 was coupled with non-diluted His6-PDZ2 and His6-Gαi1-GDP in a ratio of 1:10:3 and different incubation order with the addition of the RGS14 antibody. Immunoblot analysis was done with RGS14 antibody to Hu-RGS14 and His6 antibody to His6-PDZ2 and His6-Gαi1-GDP. (a) With the addition of non-diluted His6-PDZ2, its bindings with RGS14 were visible. While His6-Gαi1-GDP remains similar in band size, His6-PDZ2 has a stronger protein band when incubated with Hu-RGS14 first than when it was second. The asterisk* indicates the first protein being incubated with Hu-RGS14.

DISCUSSION

In the current study, we investigated the impact of the RGS14-Gαi1-GDP complex on NHERF1 binding. First, we purified and collected the proteins of interest, which includes human RGS14, NHERF1, and Gαi1-GDP. The purity of the proteins were then ensured through SDS-PAGE gels stained with Coomassie stain, showing concentrated proteins in their correct kDa size (**Fig 1&2**). Both NHERF1 and Gαi1-GDP were expressed and purified well to near homogeneity. By comparison, Hu-RGS14 was problematic in that it did not purify to homogeneity. Even so, while some impurities were present for Hu-RGS14, their minimal presence would not affect the results of complex formation analysis. A larger problem was that

the SDS-PAGE results for Hu-RGS14 size exclusion chromatography showed two peaks in the expression of Hu-RGS14, with the first peak at fractions 28-33 and the second peak at 38-45/41 (**Fig. 2**). Predicted molecular weight for purified monomeric (i.e. functional) Hu-RGS14 elutes around the size at the second peak, and we speculated the first peak being potential aggregation of human RGS14 in a non-functional dimer form. Due to the potential aggregation of Hu-RGS14 as a confounding variable, only proteins collected from fractions 38-45/41 were used to couple with NHERF1 and Gαi1-GDP with complex formation studies.

With pure protein in hand, our first studies focused on confirming interaction of Hu-RGS14 with NHERF1 and Gαi1-GDP and, at the same time, we were able to troubleshoot for different approaches and factors within the procedures. We ran into the technical problem of nonspecific binding of Hu-RGS14 to the Ni-NTA beads, which negated the negative control for Hu-RGS14 alone with Ni-NTA beads and prevented validation of the binding of NHERF1 or Gαi1-GDP with Hu-RGS14 seen in the data (**Fig. 6**). To address this, we switched tactics and immunoprecipitated the complex with an anti-RGS14 antibody, thereby eliminating the need for Ni-NTA beads. This showed that the recovered RGS14 was intact, and not cleaved. Using this approach, immunoprecipitating Hu-RGS14 with either Gαi1-GDP or NHERF1 using RGS14 antibody confirmed past studies of the interaction between Hu-RGS14 and Gαi1-GDP, suggesting a strong binding between Hu-RGS14 and Gαi1-GDP, but only a moderate interaction between Hu-RGS14 and NHERF1 (**Fig. 7**) (Friedman et al., 2022b, 2022b). Repeated attempts to observe strong NHERF1 binding were not successful.

As mentioned earlier, PDZ2 is the domain that binds to the PDZ-binding motif of Hu-RGS14 at its C-terminus (Friedman et al., 2022b). Past studies on NHERF1 have suggested that NHERF1 folds onto itself due to an intra-molecular interaction between its N-terminal PDZ2

domain and the C-terminal PDZ motif, which hinder the accessibility of the PDZ2 domain by other proteins, therefore inhibiting the association of NHERF1 with other PDZ ligands such as Hu-RGS14 (Morales et al., 2007; Sheng et al., 2012; Centonze et al., 2018). Therefore, we examined the specific binding of Hu-RGS14 to the purified PDZ2 domain and compared it to NHERF1 binding. By binding of either NHERF1 or the PDZ2 domain with Hu-RGS14 in a ratio of 3/5/10:1, PDZ2 showed a consistent binding with Hu-RGS14 when incubated with the 10:1 ratio, but NHERF1 failed to show specific binding due to its strong presence in the antibody negative control (**Fig. 8**). Despite four washes differing in level of salt and Triton X, there were no significant differences in terms of the intensity of NHERF1 binding to the antibody negative control, suggesting a potential puzzling specific binding between it and the RGS14 antibody (**Fig. 9**). One potential reason for binding so strongly to the RGS14 antibody in 10x compared to 3x in **Figure 7** could be the higher concentration, leading to a more saturated binding when only 40% of the RGS14 antibody was added in the conditions used in **Figure 8** as compared to those in **Figure 7**.

After this technical problem arose, we decided to switch our attention to the interaction between PDZ2 and Hu-RGS14, as different 10x PDZ2 showed consistent binding with Hu-RGS14 in multiple trials with successful negative controls. Because NHERF1 showed consistent non-specific binding, we used PDZ2 as an alternative option to study its interaction with Hu-RGS14 and Gαi1-GDP dimer and its role in forming a trimeric complex. When incubating 1x Hu-RGS14 with 10x PDZ2 and 3x Gαi1-GDP in different orders, we initially failed to visualize the presence of PDZ2 in the interaction while Hu-RGS14 strongly coupled with Gαi1-GDP (**Fig. 10**). This was unexpected due to consistent data suggesting a significant interaction between Hu-RGS14 and PDZ2. After increasing the concentration of PDZ2 by not diluting it with 1:2 assay

buffer as in the previous runs, the new result indicated the formation of a Hu-RGS-Gαi1-GDP-PDZ2 heterotrimreric complex (**Fig. 11**). We then asked what would happen to binding if we preformed a 1:1 complex of RGS14 with either Gαi-GDP or PDZ2. These findings suggested an interesting influence of the order of addition between PDZ2 and Gαi1-GDP. By incubating Hu-RGS14 first with PDZ2 and then Gαi1-GDP, the interaction of tri-complex formation was seen with a relatively equal proportion in the binding of the two proteins (**Fig. 11**). However, when incubating Hu-RGS14 with Gαi1-GDP first, the later coupling of PDZ2 to the dimer seemed to be significantly reduced (**Fig. 11**). By contrast, the binding of Gαi1-GDP in this context was relatively consistent with and without the addition of His6-PDZ2 (**Fig. 10&11**).

Limitation and Future Direction

While the data suggested an ordered sequence for binding to form a trimeric complex, its proper mechanisms are still limited at this point. First, with the study focusing only on the PDZ2 domain of NHERF1, the results would only be preliminary. Overall, the mechanism of the complex formation ultimately relies on knowing how NHERF1 binds in the presence or absence of bound Gαi1-GDP.

As mentioned above, NHERF1 may not bind to RGS14 when it assumes a “heads-to-tail” intramolecular folding conformation when it localizes in the cytosol (Sheng et al., 2012; Centonze et al., 2018). However, when NHERF1 is recruited to the cytoplasmic face of the plasma membrane, it changes into a relaxed conformation, which could lead to binding with RGS14 (Morales et al., 2007; Sheng et al., 2012; Centonze et al., 2018). In cells and also presumably in CA2 hippocampal neurons, the binding of Gαi1-GDP localizes and anchors RGS14 to the plasma membrane (Brown et al, 2015), and it is then in the same region where active NHERF1 would be (Harbin et al., 2021). However, if RGS14’s subcellular localization to

the plasma membrane depends on its binding of Gαi1-GDP, the current preliminary data using only the truncated PDZ2 suggests that Gαi1-GDP binding precludes trimeric complex formation. Unlike PDZ2, full-length NHERF1 may behave differently and preclude Gαi1-GDP binding. Therefore, if conditions can be determined to optimize NHERF1 binding to Hu-RGS14, future studies will examine the effects of NHERF1 binding on Gαi1-GDP binding to RGS14. First, troubleshooting for the ideal Co-IP condition or exploring new approaches, such as size-exclusion columns, would be needed to achieve that stage. As mentioned, the PDZ-motif of NHERF1 is reported to bind the PDZ2 domain of NHERF1 in an intramolecular interaction, perhaps thereby blocking PDZ2 from binding RGS14. Thus, one approach to increase full-length NHERF1 binding will be to introduce a point mutation in the PDZ-motif of NEHRF1 to block self-binding and free up the PDZ2 domain for binding RGS14 or the RGS14-Gαi1-GDP dimer. Knowing how full-length NHERF1 binds RGS14 will shed a clearer light on how these three proteins interact.

The second limitation of the study is its approach of using only purified proteins. Limiting our studies to only three pure proteins might make the interaction questionable as compared to an ideal live cell environment. While it is necessary to study in vitro, the usage of purified protein complexes can help us visualize the 3D structure of the complex between Hu-RGS14 + NHERF1 + Gαi1-GDP using Cryo-EM. Therefore, after investigating the mechanism and 3D complex structures using pure proteomic works, studying it in live cell conditions would be necessary. In this case, we will employ bioluminescence resonance energy transfer (BRET) assays in the future, allowing us to analyze protein interactions in real-time in live cells (Brown et al., 2015). Additionally, the subcellular localization of Hu-RGS14 and NHERF1 can be studied using fluorescence for detection (Shu et al., 2007).

CONCLUSION

This study examined the interaction of the RGS14-Gαi1-GDP complex with NHERF1 binding and its impact on NHERF1 binding. With a past understanding of human RGS14's involvement in hippocampal CA2 regions with various binding partners, NHERF1's interactions with human RGS14 pathways are the topic of interest in this study. With mGluR2/3, NHERF1, human RGS14, and Gαi1-GDP all present in the postsynaptic region of the human hippocampal CA2 region, we are interested in how the binding between human RGS14 with Gαi1-GDP and NHERF1 would play out in a mechanistic manner. We speculate a potential coupled interaction, perhaps as an ordered step-wise sequence of binding, since the simultaneous binding of Gαi1-GDP and NHERF1 remains unlikely due to the proximity between the GPR domain and PDZ-binding motif. Based on our working model shown in **Figure 3**, cytosolic RGS14 may bind either Gαi1-GDP to anchor itself at the plasma membrane, or it may bind NHERF1 independently to uncouple it from mGluR2/3. Alternatively, RGS14 bound at the plasma membrane by Gαi1-GDP may be uncoupled by a mGluR2/3 signaling event (e.g. phosphorylation) thereby freeing it to bind NHERF1 and uncouple it from mGluR2/3. This is similar to the proposed model of RGS14 regulation of NHERF1 in the kidney where RGS14 uncouples NHERF1 from the NPT2A transporter and phosphate uptake in GPCR-G protein (PTHR1-Gs)-dependent manner (Friedman et al, 2021). In hippocampal neurons (as in kidney), RGS14 actions could be regulated by other postsynaptic signaling events such as Ras/ERK and Ca^{++}/CaM which impact RGS14 functions. While speculative, these are important future directions to investigate.

Here, my findings provide evidence for the complexity of RGS14 binding pathways and the effect of Gαi1-GDP in the binding between human RGS14 and PDZ2 domain of NHERF1.

Further studies will test the interaction between RGS14, NHERF1, and Gαi1-GDP in both purified and live cells conditions, with new approaches such as size-exclusion columns, point mutated NHERF1, BRET assay, and fluorescence subcellular localization studies.

REFERENCES

Allen Institute for Brain Science (2004). Allen Mouse Brain Atlas [dataset]. Available from mouse.brain-map.org/gene/show/26686. Allen Institute for Brain Science (2023).

Allen Reference Atlas – Mouse Brain [brain atlas]. Available from atlas.brain-map.org.

Allen Institute for Brain Science (2004). Allen Human Brain Atlas [dataset]. Available from human. Brain-map.org. Allen Institute for Brain Science (2023).

Abd-Elrahman KS, Sarasija S, Ferguson SSG (2023) The Role of Neuroglial Metabotropic Glutamate Receptors in Alzheimer's Disease. Curr Neuropharmacol 21:273–283.

Ardura JA, Friedman PA (2011) Regulation of G Protein-Coupled Receptor Function by Na+/H+ Exchange Regulatory Factors Insel PA, ed. Pharmacol Rev 63:882–900.

Beadling C, Druey KM, Richter G, Kehrl JH, Smith KA (1999) Regulators of G protein signaling exhibit distinct patterns of gene expression and target G protein specificity in human lymphocytes. J Immunol Baltim Md 1950 162:2677–2682.

Betke KM, Wells CA, Hamm HE (2012) GPCR mediated regulation of synaptic transmission. Prog Neurobiol 96:304–321.

Blümcke I, Behle K, Malitschek B, Kuhn R, Knöpfel T, Wolf HK, Wiestler OD (1996) Immunohistochemical distribution of metabotropic glutamate receptor subtypes mGluR1b, mGluR2/3, mGluR4a and mGluR5 in human hippocampus. Brain Res 736:217–226.

Bodzęta A, Scheefhals N, MacGillavry HD (2021) Membrane trafficking and positioning of mGluRs at presynaptic and postsynaptic sites of excitatory synapses. Neuropharmacology 200:108799.

Brône B, Eggermont J (2005) PDZ proteins retain and regulate membrane transporters in

polarized epithelial cell membranes. Am J Physiol Cell Physiol 288:C20-29.

Brown NE, Goswami D, Branch MR, Ramineni S, Ortlund EA, Griffin PR, Hepler JR (2015a) Integration of G protein α (Gα) signaling by the regulator of G protein signaling 14 (RGS14). J Biol Chem 290:9037–9049.

Caruana DA, Alexander GM, Dudek SM (2012) New insights into the regulation of synaptic plasticity from an unexpected place: hippocampal area CA2. Learn Mem Cold Spring Harb N 19:391–400.

Centonze M, Saponaro C, Mangia A (2018) NHERF1 Between Promises and Hopes: Overview on Cancer and Prospective Openings. Transl Oncol 11:374–390.

Chen H, Lambert NA (2000) Endogenous regulators of G protein signaling proteins regulate presynaptic inhibition at rat hippocampal synapses. Proc Natl Acad Sci U S A 97:12810–12815.

Chevaleyre V, Piskorowski RA (2016) Hippocampal Area CA2: An Overlooked but Promising Therapeutic Target. Trends Mol Med 22:645–655.

D'Antoni S, Berretta A, Bonaccorso CM, Bruno V, Aronica E, Nicoletti F, Catania MV (2008) Metabotropic glutamate receptors in glial cells. Neurochem Res 33:2436–2443.

Evans PR, Dudek SM, Hepler JR (2015) Regulator of G Protein Signaling 14: A Molecular Brake on Synaptic Plasticity Linked to Learning and Memory. Prog Mol Biol Transl Sci 133:169–206.

Evans PR, Gerber KJ, Dammer EB, Duong DM, Goswami D, Lustberg DJ, Zou J, Yang JJ, Dudek SM, Griffin PR, Seyfried NT, Hepler JR (2018) Interactome Analysis Reveals Regulator of G Protein Signaling 14 (RGS14) is a Novel Calcium/Calmodulin (Ca2+/CaM) and CaM Kinase II (CaMKII) Binding Partner. J Proteome Res 17:1700–

1711.

Evans PR, Lee SE, Smith Y, Hepler JR (2014) Postnatal Developmental Expression of Regulator of G Protein Signaling 14 (RGS14) in the Mouse Brain. J Comp Neurol 522:186–203.

Ferraguti F, Shigemoto R (2006) Metabotropic glutamate receptors. Cell Tissue Res 326:483–504.

Friedman PA, Sneddon WB, Mamonova T, Montanez-Miranda C, Ramineni S, Harbin NH, Squires KE, Gefter JV, Magyar CE, Emlet DR, Hepler JR (2022a) RGS14 regulates PTH- and FGF23-sensitive NPT2A-mediated renal phosphate uptake via binding to the NHERF1 scaffolding protein. J Biol Chem 298:101836.

Gerber KJ, Squires KE, Hepler JR (2016) Roles for Regulator of G Protein Signaling Proteins in Synaptic Signaling and Plasticity. Mol Pharmacol 89:273–286.

Goldenstein BL, Nelson BW, Xu K, Luger EJ, Pribula JA, Wald JM, O'Shea LA, Weinshenker D, Charbeneau RA, Huang X, Neubig RR, Doze VA (2009) Regulator of G protein signaling protein suppression of Galphao protein-mediated alpha2A adrenergic receptor inhibition of mouse hippocampal CA3 epileptiform activity. Mol Pharmacol 75:1222–1230.

Harbin NH, Bramlett SN, Montanez-Miranda C, Terzioglu G, Hepler JR (2021) RGS14 Regulation of Post-Synaptic Signaling and Spine Plasticity in Brain. Int J Mol Sci 22:6823.

Harbin NH, Lustberg DJ, Hurst C, Pare J-F, Crotty KM, Waters AL, Yeligar SM, Smith Y, Seyfried NT, Weinshenker D, Hepler JR (2023) RGS14 is neuroprotective against seizure-induced mitochondrial oxidative stress and pathology in hippocampus. BioRxiv Prepr Serv Biol:2023.02.01.526349.

Häussler U, Rinas K, Kilias A, Egert U, Haas CA (2016) Mossy fiber sprouting and pyramidal cell dispersion in the hippocampal CA2 region in a mouse model of temporal lobe epilepsy. Hippocampus 26:577–588.

Hollinger S, Hepler JR (2002) Cellular regulation of RGS proteins: modulators and integrators of G protein signaling. Pharmacol Rev 54:527–559.

Hollinger S, Taylor JB, Goldman EH, Hepler JR (2001) RGS14 is a bifunctional regulator of Galphai/o activity that exists in multiple populations in brain. J Neurochem 79:941–949.

Kilias A, Tulke S, Barheier N, Ruther P, Häussler U (2023) Integration of the CA2 region in the hippocampal network during epileptogenesis. Hippocampus 33:223–240.

Lee SE, Simons SB, Heldt SA, Zhao M, Schroeder JP, Vellano CP, Cowan DP, Ramineni S, Yates CK, Feng Y, Smith Y, Sweatt JD, Weinshenker D, Ressler KJ, Dudek SM, Hepler JR (2010) RGS14 is a natural suppressor of both synaptic plasticity in CA2 neurons and hippocampal-based learning and memory. Proc Natl Acad Sci U S A 107:16994–16998.

Lin S et al. (2021) Structures of Gi-bound metabotropic glutamate receptors mGlu2 and mGlu4. Nature 594:583–588.

Millar RP, Newton CL (2010) The year in G protein-coupled receptor research. Mol Endocrinol Baltim Md 24:261–274.

Mittmann C, Chung CH, Höppner G, Michalek C, Nose M, Schüler C, Schuh A, Eschenhagen T, Weil J, Pieske B, Hirt S, Wieland T (2002) Expression of ten RGS proteins in human myocardium: functional characterization of an upregulation of RGS4 in heart failure. Cardiovasc Res 55:778–786.

Montanez-Miranda C, Bramlett SN, Hepler JR (2023) RGS14 expression in CA2 hippocampus, amygdala, and basal ganglia: Implications for human brain physiology and disease.

Hippocampus 33:166–181.

Morales FC, Takahashi Y, Momin S, Adams H, Chen X, Georgescu M-M (2007) NHERF1/EBP50 Head-to-Tail Intramolecular Interaction Masks Association with PDZ Domain Ligands. Mol Cell Biol 27:2527–2537.

Nicoletti F, Bruno V, Ngomba RT, Gradini R, Battaglia G (2015) Metabotropic glutamate receptors as drug targets: what's new? Curr Opin Pharmacol 20:89–94.

Pin JP, Duvoisin R (1995) The metabotropic glutamate receptors: structure and functions. Neuropharmacology 34:1–26.

Ritter SL, Hall RA (2009) Fine-tuning of GPCR activity by receptor-interacting proteins. Nat Rev Mol Cell Biol 10:819–830.

Ritter-Makinson SL, Paquet M, Bogenpohl JW, Rodin RE, Yun CC, Weinman EJ, Smith Y, Hall RA (2017) Group II Metabotropic Glutamate Receptor Interactions with NHERF Scaffold Proteins: Implications for Receptor Localization in Brain. Neuroscience 353:58–75.

Rosenberg N, Gerber U, Ster J (2016) Activation of Group II Metabotropic Glutamate Receptors Promotes LTP Induction at Schaffer Collateral-CA1 Pyramidal Cell Synapses by Priming NMDA Receptors. J Neurosci 36:11521–11531.

Seven AB, Barros-Álvarez X, de Lapeyrière M, Papasergi-Scott MM, Robertson MJ, Zhang C, Nwokonko RM, Gao Y, Meyerowitz JG, Rocher J-P, Schelshorn D, Kobilka BK, Mathiesen JM, Skiniotis G (2021) G-protein activation by a metabotropic glutamate receptor. Nature 595:450–454.

Sheng R, Chen Y, Yung Gee H, Stec E, Melowic HR, Blatner NR, Tun MP, Kim Y, Källberg M, Fujiwara TK, Hye Hong J, Pyo Kim K, Lu H, Kusumi A, Goo Lee M, Cho W (2012)

Cholesterol modulates cell signaling and protein networking by specifically interacting with PDZ domain-containing scaffold proteins. Nat Commun 3:1249.

Shu F, Ramineni S, Amyot W, Hepler JR (2007) Selective interactions between Giα1 and Giα3 and the GoLoco/GPR domain of RGS14 influence its dynamic subcellular localization. Cell Signal 19:163–176.

Shu F, Ramineni S, Hepler JR (2010) RGS14 is a multifunctional scaffold that integrates G protein and Ras/Raf MAPkinase signalling pathways. Cell Signal 22:366–376.

Squires KE, Gerber KJ, Pare J-F, Branch MR, Smith Y, Hepler JR (2018) Regulator of G protein signaling 14 (RGS14) is expressed pre- and postsynaptically in neurons of hippocampus, basal ganglia, and amygdala of monkey and human brain. Brain Struct Funct 223:233–253.

Talbot JN, Jutkiewicz EM, Graves SM, Clemans CF, Nicol MR, Mortensen RM, Huang X, Neubig RR, Traynor JR (2010) RGS inhibition at G(alpha)i2 selectively potentiates 5-HT1A-mediated antidepressant effects. Proc Natl Acad Sci U S A 107:11086–11091.

Traver S, Bidot C, Spassky N, Baltauss T, De Tand MF, Thomas JL, Zalc B, Janoueix-Lerosey I, Gunzburg JD (2000) RGS14 is a novel Rap effector that preferentially regulates the GTPase activity of galphao. Biochem J 350 Pt 1:19–29.

Tzakis N, Holahan MR (2019) Social Memory and the Role of the Hippocampal CA2 Region. Front Behav Neurosci 13 Available at: https://www.frontiersin.org/articles/10.3389/fnbeh.2019.00233 [Accessed March 15, 2023].

Vatner DE, Zhang J, Oydanich M, Guers J, Katsyuba E, Yan L, Sinclair D, Auwerx J, Vatner SF (2018) Enhanced longevity and metabolism by brown adipose tissue with disruption of

the regulator of G protein signaling 14. Aging Cell 17:e12751.

Vellano CP, Brown NE, Blumer JB, Hepler JR (2013) Assembly and Function of the Regulator of G protein Signaling 14 (RGS14)·H-Ras Signaling Complex in Live Cells Are Regulated by Gαi1 and Gαi-linked G Protein-coupled Receptors. J Biol Chem 288:3620–3631.

Vinson PN, Conn PJ (2012) Metabotropic glutamate receptors as therapeutic targets for schizophrenia. Neuropharmacology 62:1461–1472.

Zhao M, Choi Y-S, Obrietan K, Dudek SM (2007) Synaptic Plasticity (and the Lack Thereof) in Hippocampal CA2 Neurons. J Neurosci 27:12025–12032.

Zheng B, De Vries L, Gist Farquhar M (1999) Divergence of RGS proteins: evidence for the existence of six mammalian RGS subfamilies. Trends Biochem Sci 24:411–414.